



Unusual enhancement in tropospheric and surface ozone due to orography induced gravity waves

D.V. Phanikumar^{a,*}, K. Niranjana Kumar^b, S. Bhattacharjee^a, M. Naja^a, I.A. Girach^c, Prabha R. Nair^c, Shweta Kumari^d

^a Aryabhata Research Institute of Observational Sciences, Nainital, India

^b Atmosphere and Ocean Research Institute, The University of Tokyo, Chiba, Japan

^c Space Physics Laboratory, Vikram Sarabhai Space Centre, Thiruvananthapuram 695022, India

^d Indian School of Mines, Dhanbad, Jharkhand, India



ARTICLE INFO

Article history:

Received 10 April 2017

Received in revised form 28 June 2017

Accepted 15 July 2017

Available online xxxx

Keywords:

Ozone

Tropopause

Orographic waves

Propagation

ABSTRACT

In this study, we investigate the causative processes responsible for the observed enhancement in the tropospheric and surface ozone during December 09–11, 2008 orography induced gravity wave event over Himalayan region. The analysis is done using surface ozone measurements and satellite datasets from Atmospheric Infrared Sounder/Advanced Microwave Sounding Unit-A (AIRS/AMSU-A), COSMIC, TES and Cloud-Aerosol Lidar and Infrared Pathfinder Satellite Observation (CALIPSO). Observations depict a two fold increase in surface and tropospheric ozone during the event as compared to normal days in both AIRS and TES ozone measurements. COSMIC temperature perturbations show generation of shorter vertical wavelengths efficient for the sub-tropical tropopause folding due to orography induced gravity waves. Moreover, the intense tropopause folding as evidenced by upward-downward vertical velocities couplet could trigger the intrusion of stratospheric ozone rich air into upper tropospheric ozone poor air as also confirmed by high values of potential vorticity during the observational period. Hence, present study reemphasizes the importance of wave induced atmospheric dynamics on atmospheric constituents' especially tropospheric ozone over Himalayan region.

© 2017 Elsevier Inc. All rights reserved.

1. Introduction

Ozone is one of the most important atmospheric trace gas in both stratosphere and troposphere affecting the Earth-atmosphere radiative balance and hence the climate (Cracknell and Varotsos, 2011). The stratospheric ozone constituting about 90% of total ozone concentration in the atmosphere, although very small amounts as compared to other gases, protects life on earth by blocking harmful UV radiation reaching surface (Cracknell and Varotsos, 1994, 1995; Varotsos and Cracknell, 1994). On the other hand, tropospheric ozone, constituting to only ~10% of total ozone in the atmosphere, found to be having adverse effects on vegetation as well as on human health (Zeng et al., 2008; Kumar et al., 2010; Lelieveld et al., 2015). Although, very less in concentration but tropospheric ozone happens to be third most powerful greenhouse gas (after carbon-dioxide and methane) with radiative forcing of $0.40 \pm 0.20 \text{ W m}^{-2}$ (IPCC, 2013). Thus, increase (decrease) in tropospheric (stratospheric) ozone is of recent interest to the scientific community because of enormous impact on the society, especially, on human health related issues like irritation in respiratory system,

reduction in the efficiency of the lung function, aggravations in asthma etc. Tropospheric and surface ozone showed increasing trend over most of the locations in Indian region (Naja and Lal, 1996; David and Nair, 2013). Moreover, a recent report showed tropospheric ozone causes roughly 22,000 premature deaths per year in 25 countries in European Union (WHO, 2012). It is imperative that if the percentage of contribution of tropospheric ozone increase could result in fourfold increment in the death figures in Indo Gangetic plain region because of heavy population density (Lelieveld et al., 2015). Ghude et al. (2016) has also estimated the mortality rate by chronic obstructive pulmonary disease (COPD) due to O_3 exposure is about 12,000 people on a national scale. Hence, it is crucial to understand different processes responsible for the enhancement of tropospheric ozone over local, region and global scales.

The photochemistry involving different trace gases largely emitted from various anthropogenic sources (e.g. motor vehicle exhaust, industrial emissions, etc.), controls the ozone budget (e.g. Kumar et al., 2013). It has been shown that the transport of ozone rich air from polluted regions to pristine high altitude or marine regions (Chand et al., 2001; Naja et al., 2004; Lal et al., 2013; Girach et al., 2017) could influence ozone budget in those regions. Further, greater uncertainties exists in the downward transport of ozone and dry deposition process

* Corresponding author.

E-mail address: phani@aries.res.in (D.V. Phanikumar).

(Stevenson et al., 2006). Downward transport of ozone has been suggested to have contribution in higher levels of ozone during winter/spring at a number of sites across the globe and about 0.1% of total stratospheric ozone (about 5×10^{13} molecules $\text{cm}^{-2} \text{s}^{-1}$) is suggested to be transported to the troposphere (e.g. Logan, 1985; Crutzen, 1995; Ojha et al., 2014; Sarangi et al., 2014). Stratospheric-ozone intrusions into the troposphere during events of cyclones also been observed over Indian regions (Das et al., 2016a, 2016b).

Past studies showed that ozone enters into troposphere from stratosphere by means of large scale phenomena as a part of Brewer Dobson Circulation triggered by a variety of processes (Levy et al., 1985; Holton et al., 1995; Hocking et al., 2007; Chen et al., 2011; Nath et al., 2016). Moreover, this large-scale circulation is one of the most important contributors for the enhancement in the tropospheric ozone in extra-tropical latitudes (Holton et al., 1995; Nath et al., 2016). Recent study showed that an increasing trend and westward shift of number of intrusions contributing to the increased tropospheric ozone over the central Pacific (Nath et al., 2016). The episodes of downward intrusion of stratospheric air (dry air causing low humidity) are, in general, associated with the behaviour of subtropical jet stream and these are strongest in winter over the Himalayan region and hence the intrusion of air masses from the stratosphere may contribute to higher upper tropospheric ozone in winter than in summer leading to an additional radiative impact over Tibetan Plateau (Chen et al., 2011; Naja et al., 2016; Niranjana Kumar et al., 2016). It is also worth mentioning here that previous reports showed that the frequent laminated vertical ozone structures over sub-tropical latitudes are related to atmospheric circulation phenomena (Varotsos et al., 1994). Additionally, Tobo et al. (2008) showed that high ozone stratospheric intrusion into troposphere is closely associated with the tropopause folds and the frequencies of these folds directly linked with stratospheric intrusions and vertical distribution of ozone over Himalayan region. In this context, it has become mandatory to quantify various factors contributing to the tropospheric ozone and once such dynamical episodic event outlined in the present report.

Furthermore, satellite observations showed that “ozone mini-hole” events are transporting ozone from troposphere (ozone poor) into stratosphere (ozone rich) through tropopause during summer season over the Himalayan region (Zhou and Zhang, 2005; Tobo et al., 2008; Bian, 2009). However, during winter and early spring, stratospheric (ozone rich) intrusions into troposphere (ozone poor) are more frequent thereby injecting the ozone into upper and lower troposphere. In this perspective, it is essential to understand and quantify the plausible reasons for intrusion of stratospheric ozone into troposphere which has immense impact on atmospheric radiation budget over Himalayan region.

Very few studies in the recent past highlighted the importance of vertically propagating disturbances/gravity waves propagating to tropopause especially during tropical cyclone events could result in stratosphere-troposphere exchange (STE) process. These studies emphasized the potential of wind profiler radars by providing observational evidence of stratospheric ozone intrusions into troposphere as a part of campaign mode and also during tropical cyclone events (Hocking et al., 2007; Das, 2009; Niranjana Kumar and Ramkumar, 2008; Niranjana Kumar et al., 2011; Das et al., 2016a, 2016b; Pathakoti et al., 2016). On the other hand, mountain waves are not so frequent but will have high amplitudes when these waves are triggered over the Himalayan region where some of the highest mountains on earth are located causing hindrance to the horizontal wind flow thereby setting up of oscillations. These waves have the potential to show signatures not only to upper troposphere but also to stratosphere and mesosphere. However, it is based on the strength of the initial disturbance, and under suitable meteorological conditions, these waves are capable for vertical propagation (Niranjana Kumar et al., 2012; Lyapustin et al., 2014; Kim et al., 2016; Kaifler et al., 2015). Hence, recent studies around the globe have opened up a new window not only illustrating the

importance of vertical forcing in quantifying the tropospheric ozone but also gave a strong message that vertically propagating disturbances/gravity waves cannot be neglected keeping in mind the importance of STE processes on day-to-day basis.

In view of the above scenario, present study for the first time attempts to understand the enhancement of tropospheric and surface ozone by means of STE process triggered by orography induced atmospheric gravity waves over Himalayan region. This study utilizes different satellite datasets such as Microwave Limb Sounder (MLS), Atmospheric Infrared Sounder/Advanced Microwave Sounding Unit-A (AIRS/AMSU-A), COSMIC temperature perturbations, Tropospheric Emission Spectrometer (TES) on board Aqua satellite, and Cloud-Aerosol Lidar and Infrared Pathfinder Satellite Observation (CALIPSO) to understand the impact of mountain waves on the unusual enhancement in the tropospheric ozone during December 2008 over the Himalayan region. In the following sections, we have identified the mountain waves through AIRS observations and established the link between mountain waves and ozone transport. Finally, we have discussed the plausible mechanism responsible for the stratospheric ozone intrusion into upper troposphere causing unusual enhancement in tropospheric and surface ozone over the Himalayan region.

2. Data used

The present study utilizes the data from AMSU-A and AIRS sounders on board the National Aeronautics and Space Administration (NASA) Aqua satellite. Tropospheric and stratospheric temperature sounding is done using twelve channels covering 50 to 60 GHz oxygen band. In this study, we have used the raw radiance measurements, from 53.6 GHz channel with weighting function peaks at ~ 600 hPa, to identify the gravity wave perturbations in the troposphere (Aumann et al., 2003). The methodology used for the retrieving the radiance perturbations are closely followed from Niranjana Kumar et al. (2012). In this study, we make use of the AIRS (level-2 and level-3) version-6 ozone, temperature, and humidity information at different pressure levels. More technical details and retrieval of surface and atmospheric parameters of the AIRS/AMSU system can be found elsewhere (Aumann et al., 2003; Susskind et al., 2003). As a supplement to the utilization of AIRS/AMSU measurements, the along track tropopause height from CALIPSO data provided by the Global Modeling and Assimilation Office (GMAO) data assimilation system is also utilized.

The dynamical analysis, in support of AIRS/AMSU observations, is done using the European Centre for Medium Range Weather Forecasts (ECMWF) interim Re-Analysis (ERA) data (Dee et al., 2011). ERA-interim products are available on the ECMWF data server at various spatial (latitude, longitude) resolutions at 37 pressure levels from 1000 to 1 hPa. In the present analysis, we have used the vertical (pressure) velocities and potential vorticity fields at 1.5×1.5 degree spatial intervals.

We have utilized Constellation Observing System for Meteorology, Ionosphere and Climate (COSMIC) temperature profiles during December 07–11, 2008 to estimate the vertical wavelengths generated due to orographic generated gravity waves over Himalayan region. COSMIC is a Taiwan-US joint mission with a constellation of six microsatellites equipped with GPS receivers and provides ~ 2500 occultations per day over the globe. COSMIC satellites were launched in early 2006 and providing continuous data from April 2006, however, coverage is low over equatorial region. Further details about COSMIC mission can be found in earlier papers (Kursinski et al., 1997; Anthes et al., 2008). In the present study, COSMIC level 2 temperature profiles are chosen nearest to the latitude (longitude) belt of $35\text{--}45^\circ\text{N}$ ($65\text{--}75^\circ\text{E}$) which is the region of intense mountain wave activity. Data points flagged with bad quality are not considered for the analysis.

Tropospheric Emission Spectrometer (TES) ozone is on the Aura satellite which has a ~ 705 km sun-synchronous polar orbit with an equator crossing time of $\sim 13:45$ and a 16-day repeat cycle was designed to measure the global vertical distribution of tropospheric ozone, as well as

temperature and other important tropospheric species including carbon monoxide, methane and water vapor (Beer et al., 2001; Beer, 2006). TES ozone is retrieved from the 9.6 μm ozone absorption band using the 995–1070 cm^{-1} spectral range. The retrievals and error estimation are explained in detail in earlier papers (Rodgers, 2000; Worden et al., 2004; Bowman et al., 2006; Kulawik et al., 2006).

2.1. Surface ozone

Observations of surface ozone were carried out during December 2008 at Nainital (NTL) and Trivandrum (TVM) using UV photometric ozone analysers of Environment S.A. (model O341M), France and Thermo Electron Corporation (model 49C), USA respectively. These analysers measure the ozone mixing ratio based on the principle of absorption of ultraviolet radiation (wavelength ~ 254 nm) by the ozone molecules utilizing Beer–Lambert's law. Air sample is drawn through a teflon tube and passed through a teflon filter to remove aerosol particles before entering the instrument. The analysers have lower detection limit of 1 ppbv. The accuracy of these instruments is reported to be about 5% (Kleinman et al., 1994). A detailed instrumental description of the analyser is given in Kumar et al. (2010) and David and Nair (2011).

3. Results

Fig. 1 shows the map of Indian sub-continent highlighting the two observational sites Manora Peak, Nainital (29.4°N , 79.5°E , 1958 m amsl) and equatorial location Thumba, Trivandrum (8.5°N , 76.9°E , 3 m amsl), respectively. The plains of the Ganges Valley lie approximately 50 km to the south, and higher altitude mountains (4 km amsl) of the Himalayan Ranges lie to the north. The site is located well away from large/small scale industrial and population centers, and considered to be cleaner site in terms of air pollution as compared to other major cities. The mega city of Delhi, capital of India, is located about 225 km to the southwest. A detailed description of the topography and general meteorology of the observational site is discussed in previous papers (for e.g. Shukla et al., 2014). On the other hand, the measurement site Thumba is situated ~ 500 m away from the Arabian Sea coast in the city of Trivandrum. It has sandy terrain and surrounded by less populated area. The sea-breeze/land breeze activity, which controls diurnal variation of ozone, prevails over the site throughout the year.

Fig. 2a–b shows radiance perturbations (53.6 GHz) at 600 hPa (chosen to visualize the wave perturbations in the tropospheric heights) on December 09, 2008 at 07:59:25 UT and 21:41:25 UT for both ascending

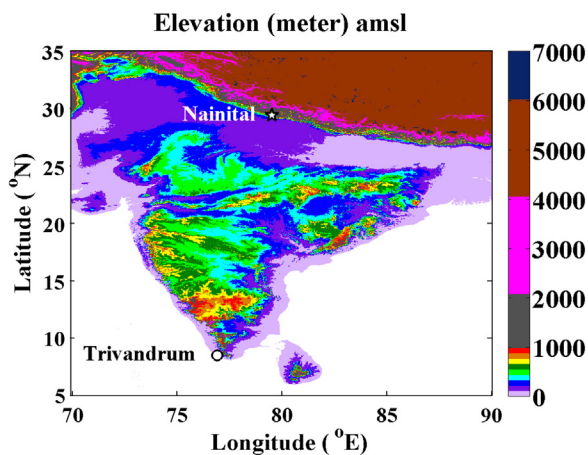


Fig. 1. Latitude-longitude elevation map of Indian region showing both Nainital (29.4°N , 79.5°E , 1958 m amsl) in Central Himalayan region and Trivandrum (8.5°N , 76.9°E , 3 m amsl) and the locations are represented by star and circle, respectively.

and descending passes, respectively as obtained from AMSU-A. It is clearly evident from the figure that wave perturbations are prominent in the troposphere (at 600 hPa) in both the passes over Himalayan region ($30\text{--}40^\circ\text{N}$; $60\text{--}90^\circ\text{E}$). The observed phase lines of the waves are aligned in northwest and southwest directions in both ascending and descending passes. It is also noteworthy that these wave perturbations are observed with similar amplitudes in both ascending and descending passes indicate that these waves would have persisted for more than a day or two and also confirming that the modulations originate from topographic wind-flow associated with strong flow across the mountain terrain region usually termed as mountain waves (Durran, 1986). Our earlier study (Niranjan Kumar et al., 2012) estimated the horizontal (zonal; meridional) and vertical wavelengths which turned out be (276 km; 289 km) and 25 km, respectively. A comprehensive picture of the stratospheric effect of this mountain wave event is explained and discussed in detail by Niranjan Kumar et al. (2012). A further analysis on the same event is carried out in the present study to expose the effect of these wave perturbations not only on lower stratospheric and upper tropospheric but also on surface ozone concentration over Himalayan region as this event is very special in terms of intense and persistent mountain wave perturbations.

Fig. 2c–d shows the pressure-longitude cross section of vertical velocities during December 09, 2008 at 06 and 18 UT, respectively at $\sim 32.5^\circ\text{N}$ latitude. Positive (negative) velocities corresponds to downward (upward) velocities. It is interesting to note that strong updrafts ($> 1 \text{ m s}^{-1}$) could be potential indicators of dynamical processes associated with gravity waves due to topographic wind flow followed by strong downdrafts over $60\text{--}80^\circ\text{E}$ longitude belt at tropopause altitudes indicating the possible intrusion of lower stratospheric air into upper troposphere air. In general perspective, the vertical velocities will be more in lower troposphere during convective conditions. Nevertheless, during the mountain wave event, these waves propagated vertically to higher heights which is evident with the observed strong updrafts (due to exponential decrease in the density).

Since, we are dealing with ozone transport and temperature gradients in the lower stratosphere and upper tropospheric heights at subtropical latitudes, we utilize the tropopause pressure and height data from AIRS and CALIPSO, respectively during the mountain wave event. Fig. 3a–d shows the latitude-longitude map of tropopause pressure derived from AIRS during (a) December 08, 2008 at 08:59:25 UT, (b) December 09, 2008 at 21:41:25 UT, (c) December 10, 2008 at 20:47:25 UT, (d) December 11, 2008 at 21:29:25 UT and latitudinal variation of tropopause pressure/height derived from CALIPSO data are plotted for December 09 & 11, 2008 to understand the effect of mountain waves on the tropopause height/pressure (Fig. 3e). Interestingly, on December 09, 2008 tropopause height (pressure) has drastically decreased (increased) from ~ 16 km (100 hPa) to ~ 10 km (250 hPa) leading to an intense tropopause folding within the box region at a short span of 2–3 degree latitude triggered by the mountain wave event as compared to other non-event days. In this context, it is worth mentioning here that the intense tropopause folds are generally associated with stratosphere-troposphere exchange process and also the ozone intrusion into upper troposphere may be prominent depending upon different levels of excursion (Hocking et al., 2007).

In order to confirm the plausible reasons for the tropopause folding and its significance, power spectrum (Fourier transform and wavelet) temperature perturbations of COSMIC GPS RO during December 07–11, 2008 profiles are used shown in Fig. 4. The shading plots in the figure represent the normalized wavelet power spectrum as a function of height. The x-axis represents the height and y-axis represents the vertical wavelength. The significance powers at 99% confidence for vertical wavelengths are encompassed with the contours. The COSMIC Radio occultations are chosen nearest to the region of intense mountain wave activity between $30\text{--}40^\circ\text{N}$ and $65\text{--}75^\circ\text{E}$. It is clearly evident from the figure that shorter vertical wavelength gravity waves (below 6 km) are prominent during December 09, 2008 mountain wave event as

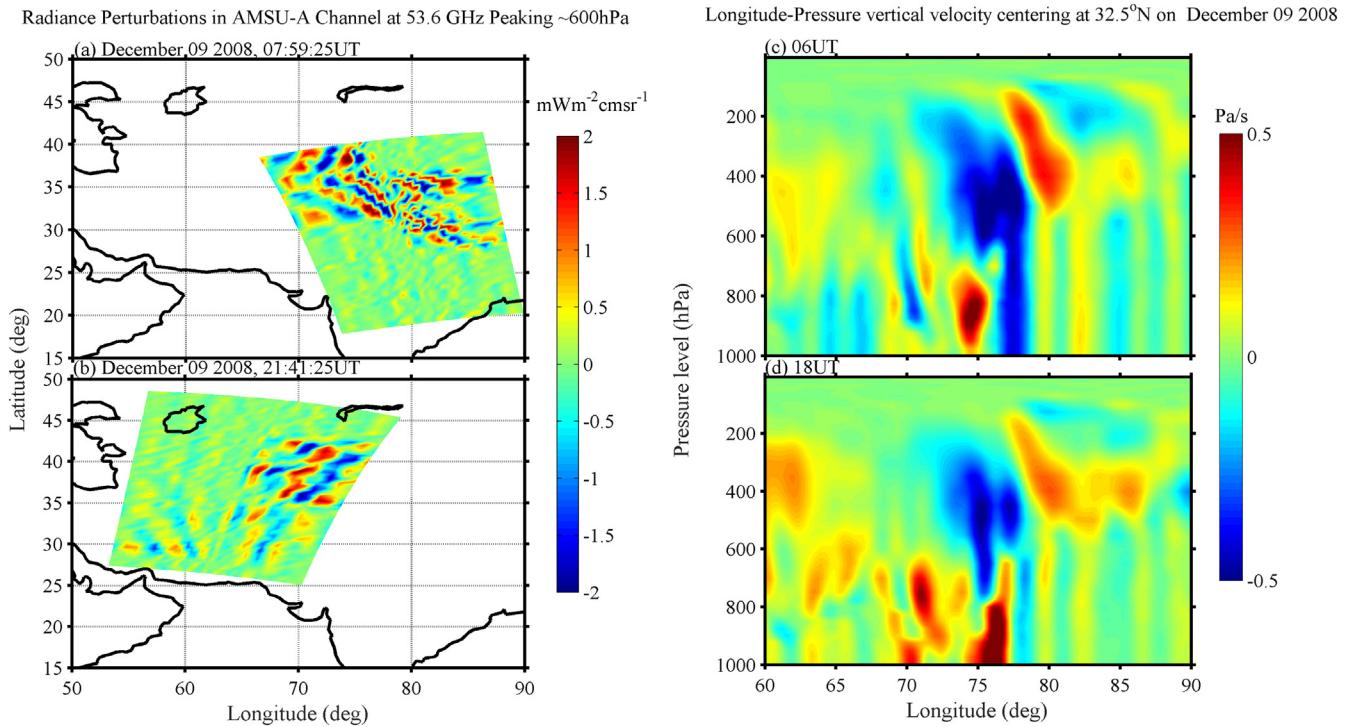


Fig. 2. (a–b) Radiance perturbations of AMSU-A channel onboard NOAA polar satellite at 53.6 GHz peaking at 600 hPa (chosen to visualize the wave perturbations in the lower tropospheric heights) on December 09, 2008 at 07:59:25 UT and 21:41:25 UT for both ascending and descending passes. (c–d) Pressure–longitude variation of vertical velocities derived from ECMWF re-analysis datasets during December 09, 2008 at 06 and 18 UT, respectively at 32.5°N latitude. Positive (negative) velocities corresponds to downward (upward) velocities.

compared to other days indicating the efficiency of these wave breaking at the tropopause level can lead to tropopause folding which also reflects from the estimates of CALIPSO tropopause pressure/height (Fig. 3). Interestingly, wavelet power spectrum depicts similar picture showing the dominance of shorter vertical wavelength gravity waves at the tropopause level reconfirming the tropopause folding by the mode of wave breaking at those levels. However, these shorter wavelength gravity waves are not so efficient in the stratosphere as they deposit their energy within troposphere due to damping mechanism (Dhaka et al., 2006). It is also worth mentioning here that the wave breaking can occur through convective instability and more likely in orography generated gravity waves as evidenced in earlier reports (Fritts and Rastogi, 1985; Lamarque et al., 1996). To support this argument further, Efsthathiou and Varotsos (2010) showed that the temperature fluctuations are increasing with increase in altitude in the lower troposphere and these perturbations will have maximum amplitude at tropopause altitudes.

Fig. 5a–d illustrates the latitude–longitude map of ozone mixing ratios during December 08–11, 2008 at respective timings for two pressure levels 250 and 300 hPa, respectively obtained from AIRS. The reason for choosing these two pressure levels is to understand the ozone distribution in upper tropospheric levels based on rise in tropopause pressure (~250 hPa) during the mountain wave event. It is clearly evident from the figure that almost two fold enhancement in upper tropospheric ozone during the mountain wave event (December 09 and 10) as compared to normal days (December 08 and 11), where increase in tropospheric ozone is not observed.

Tropospheric ozone averaged between 100 and 300 hPa during December 09, 2008 (mountain wave event) is around 0.15 ± 0.01 ppmv (150 ± 10 ppbv) as compared to December 11, 2008 (normal day) which is around 0.05 ± 0.002 ppmv (50 ± 2 ppbv) traversing further down to upper and mid-troposphere during subsequent days. Longitudinal cross section also depicting similar variation but the transport is observed from 60°E to 100°E longitudes. Interesting to note that the ozone amplitudes are intense over latitudes (longitudes) covering

30°N–40°N (60°E–80°E) which are exactly coinciding with the region of intense mountain wave activity during that period (see Fig. 2). On December 11, 2008, decay in amplitudes is observed and reached to almost normal situation, however, still small percentages of upper tropospheric ozone are seen keeping in mind the ozone photochemistry and other production/transport contributions but overall it is much less as compared during the mountain wave activity days.

To see the spatial extent of enhanced ozone mixing ratio at various pressure levels, latitude–longitude maps of ozone for different pressure (70–300 hPa) on December 09, 2008 at 21.41.25 UT as shown in Fig. 6a–f. The higher ozone mixing ratios (>1.5 ppm) in the stratosphere at 70 hPa are clearly observed. For upper and mid troposphere ozone values are ~150 ppbv (at 300 hPa). The intrusion of ozone from lower stratosphere to upper troposphere is clearly visible from 70 to 300 hPa pressure levels contributing to the unusual enhancement in the tropospheric ozone although small as compared to stratospheric ozone concentration but significant while considering the adverse effects within the increase of tropospheric ozone. It is also worth mentioning here that despite different passes on different days depict the intense intrusion of stratospheric ozone into mid-troposphere around 30–40°N latitude and 60–80°E longitude belts signifying the spatial extent of these mountain waves over the Himalayan region.

Further, to reconfirm the intrusion of stratospheric ozone rich air into tropospheric ozone poor air, pressure time cross section of potential vorticity (PV) (good indicator for stratosphere-troposphere intrusions) and relative humidity during December 08–12, 2008 at a specific location (35°N, 72°E) are plotted in Fig. 7a–b. The high PV values in general are associated with strong static stability and within the troposphere PV values are usually less ($PV < 1$ PVU (potential vorticity unit); $1 \text{ PVU} = 10^{-6} \text{ km}^2 \text{ kg}^{-1} \text{ s}^{-1}$) because of weak stability, however, stratospheric PV values could go as high as 4 PVU. Hence, intrusions can be easily identified if high values of PV are observed (mostly $PV > 1$ PVU) in the troposphere which are associated with lower stratospheric air (larger static stability) descending down to upper troposphere (Hoskins et al., 1985). It is interesting to note that high PV values

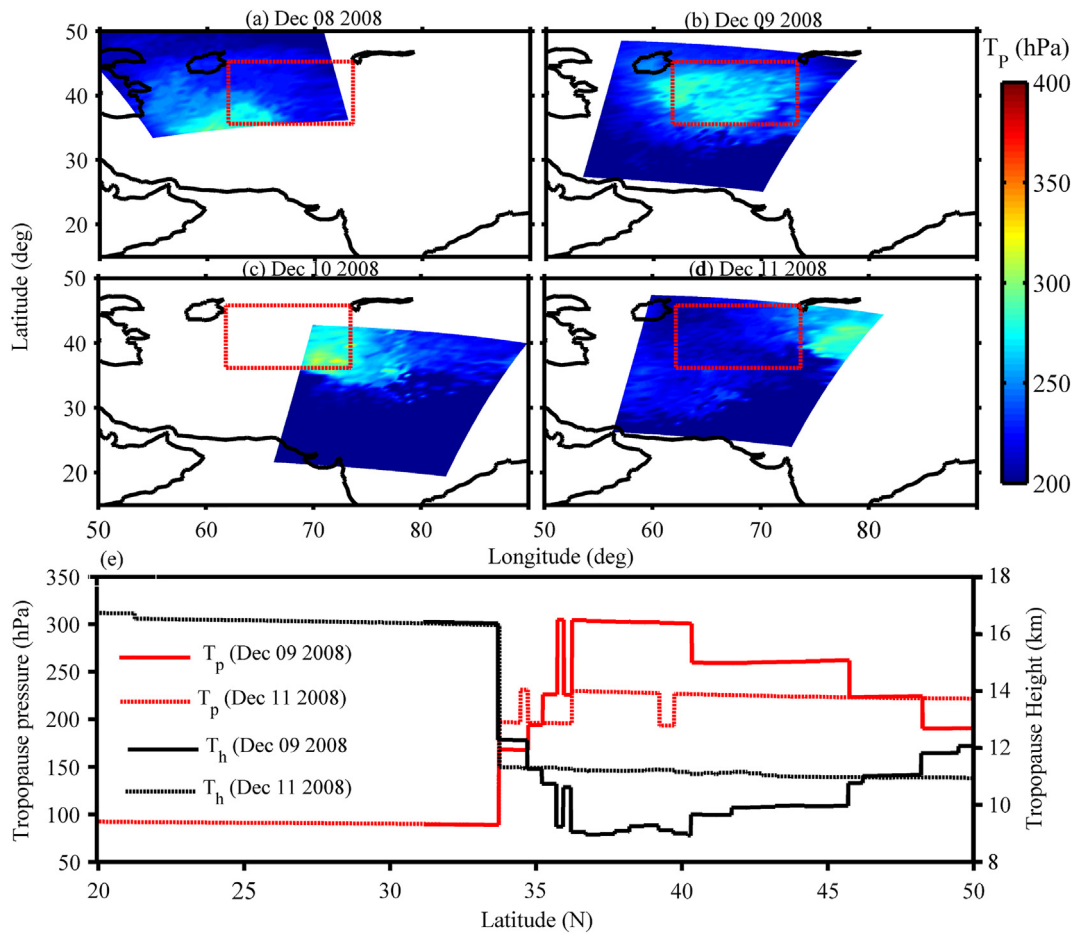


Fig. 3. Latitude-longitude map of AIRS tropopause pressure for (a) December 08, 2008 at 08:59:25 UT, (b) December 09, 2008 at 21:41:25 UT, (c) December 10, 2008 at 20:47:25 UT, (d) December 11, 2008 at 21:29:25 UT; (e) latitudinal variations of tropopause pressure/height derived from CALIPSO/CALIOP data are plotted during December 09 & 11, 2008 centering on $70^\circ \pm 5^\circ$ longitude belt.

(PVU > 1.2) are extended downwards during the mountain wave event to even 600–700 hPa indicating strong intrusions of dry air from lower stratosphere to mid troposphere. However, there are no such PV values

observed on other days during our observational window indicating that the intrusions might be associated with the mountain wave activity. Moreover, relative humidity values also showing low values during

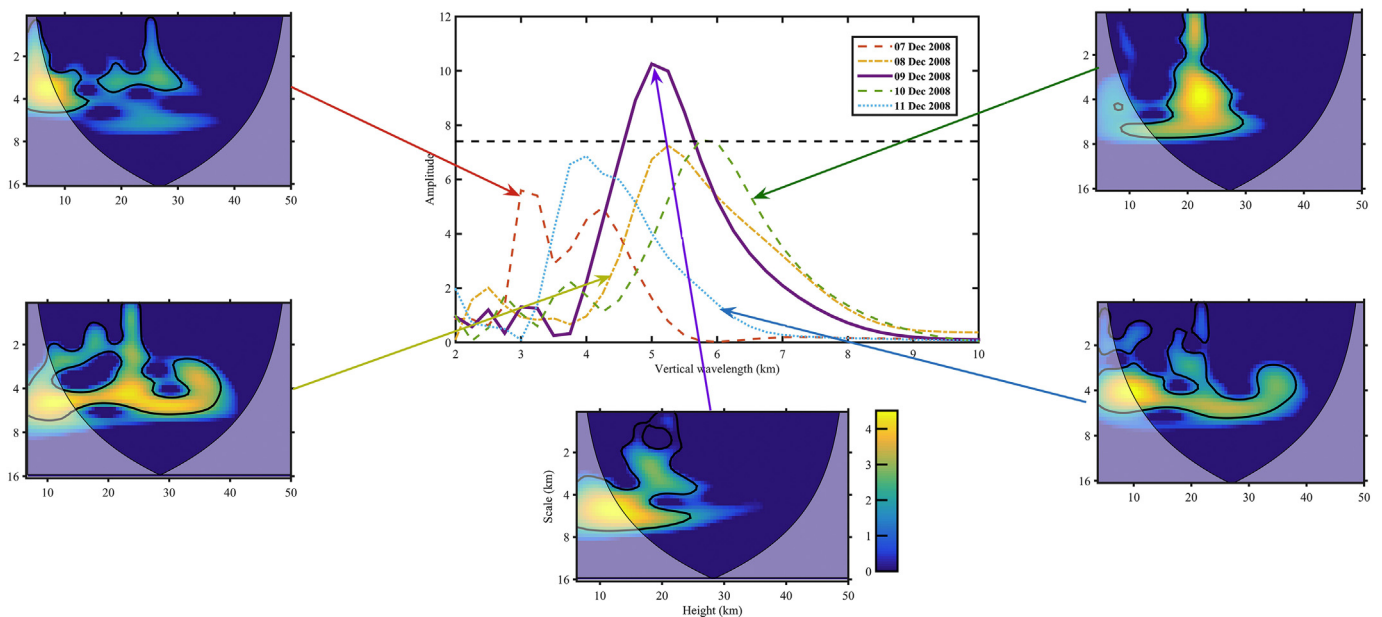


Fig. 4. Wavelet power spectrum in units of % normalized variance of COSMIC temperature perturbations during December 07–11, 2008 mountain wave event. Horizontal dotted line represents 99% significance level.

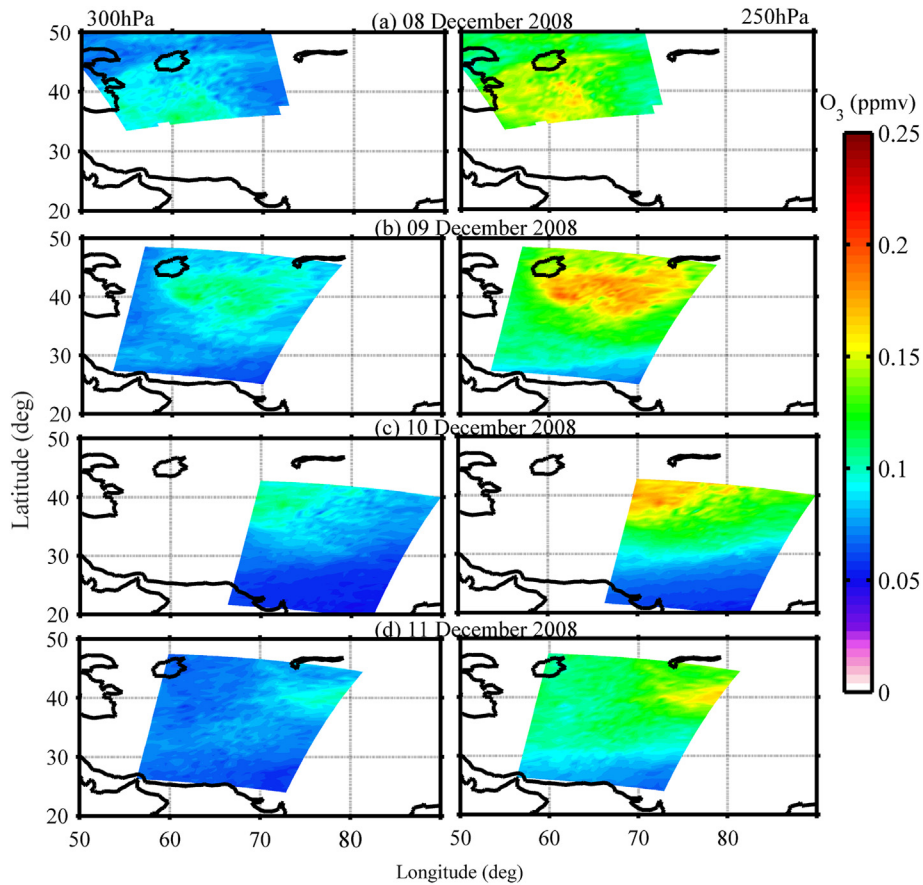


Fig. 5. a–d: Latitude-longitude map of AIRS mean ozone mixing ratio (ppmv) for December 08, 2008 at 08:59:25 UT; December 09, 2008 at 21:41:25 UT; December 10, 2008 at 20:47:25 UT; December 11, 2008 at 21:29:25 UT for 250 and 300 hPa pressure levels, respectively.

the event day in the mid- and upper troposphere reconfirming that dry stratospheric ozone rich air entering into humid troposphere enhancing the tropospheric ozone concentration.

Finally, in order to visualize the downward propagation of ozone concentration, surface ozone over NTL and TVM; AIRS ozone concentration at 300 hPa; and tropopause temperature are plotted with time during December 01–21, 2008 as depicted in Fig. 8 It is clearly evident from the figure that surface ozone is showing almost two fold enhancement whereas such variation is not observed over Trivandrum although far but plain site (free from mountain terrain). As per the average surface

ozone values in December month is around 30 ppbv or below considering the high altitude location like Nainital, considered to be free from local pollution and having good air quality conditions (Kumar et al., 2011). In comparison to the surface ozone, AIRS ozone at 300 hPa averaged over Nainital region (29–30°N and 79–80°E) showing enhancement during the same event. It is also interesting to note that both surface and ozone at 300 hPa are showing significant increase during the mountain wave event indicating the influence of these waves on the ozone downward transport. Absence of enhancement over Trivandrum points that this event has affected the surface ozone on regional

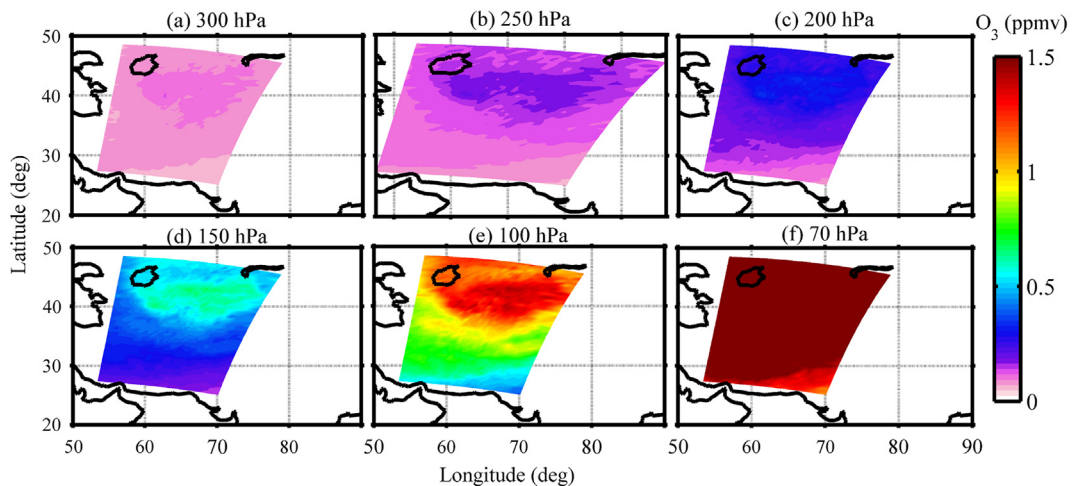


Fig. 6. a–d: Latitude-longitude map of AIRS mean ozone mixing ratio (ppmv) for different pressure levels (a) 300 hPa, (b) 250 hPa, (c) 200 hPa, (d) 150 hPa, (e), 100 hPa and (f) 70 hPa (lower panel) on December 09, 2008 at 21:41:25 UT.

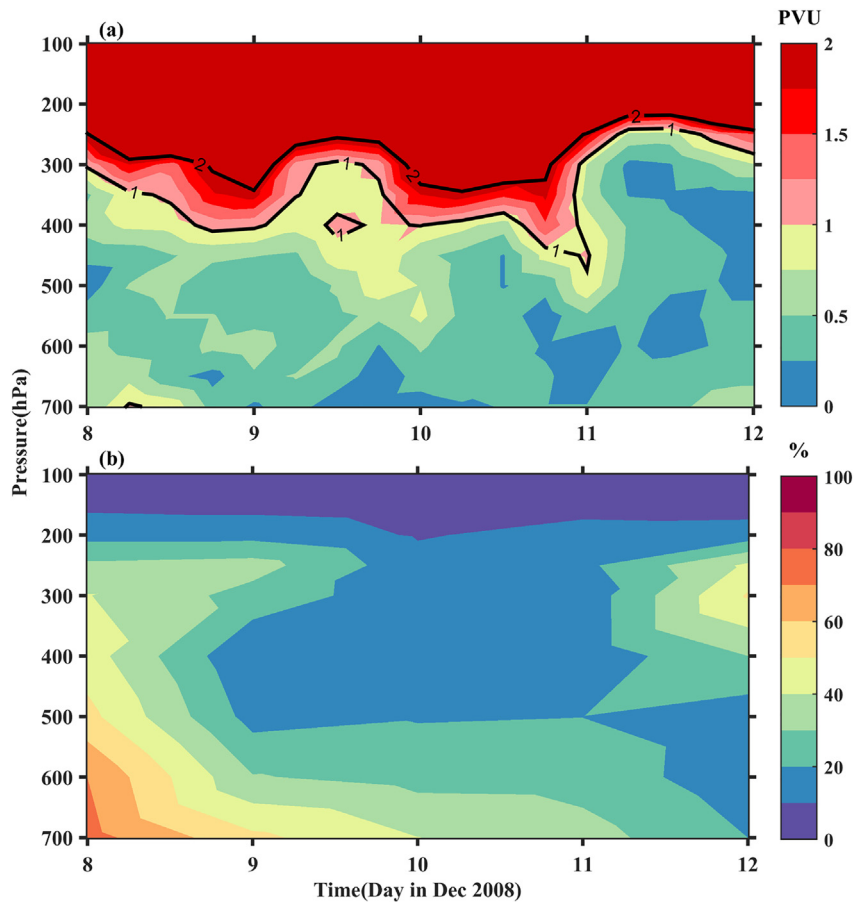


Fig. 7. a–b: Pressure-time cross section of potential vorticity (PV) and relative humidity during December 08–12, 2008 at a specific location where the intrusions were maximum (35°N , 72°E).

scale but not the larger region. It can further be inferred that tropospheric ozone budget is highly region dependent.

In the present study, surface ozone values were ~ 58 ppb for two consecutive days. This points out that the air quality (considering ozone alone) can be poor occasionally over high altitude locations under such events of stratospheric intrusion of ozone into the lower troposphere. Considering tropopause height of ~ 10 km on December 09,

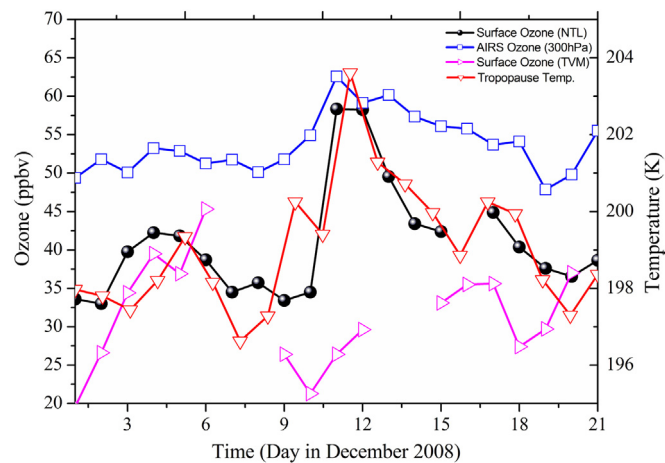


Fig. 8. Temporal evolution of AIRS ozone at 300 hPa (blue) averaged over Nainital region, daily surface ozone at Nainital (black), daytime surface ozone at Trivandrum (magenta) and tropopause temperature (red) over Nainital region during December 01–21, 2008. (For interpretation of the references to colour in this figure legend, the reader is referred to the web version of this article.)

2008, and say ozone-rich air mass takes ~ 2 days to reach at Nainital altitude (~ 2 km) and enhancement in surface ozone was observed on December 11, 2008. Based on this, we estimate mean descent rate of ozone to be ~ 4 km/day in the troposphere. The stronger intrusion had occurred at higher latitudes (35° – 45°N) compared to the Nainital latitude (29°N) on December 09, 2008 and hence descent of ozone is not vertically straight but it has horizontal component which would lead to even faster descent rate than what is reported here. However, the descent rate is approximately 4 times higher what is reported by Das et al. (2016a, 2016b) during cyclone events. Interestingly, similar intrusion is clearly observed in TES ozone data on December 09, 2008 at higher latitudes indicating that the event may have triggered due to orography induced gravity waves (see Fig. S1). Now, considering the intrusion on December 09, 2008 might have reached Nainital on December 11, 2008 showing the enhancement in the surface ozone values in Nainital (located in central Himalayan region).

4. Discussion

Although few studies focused on the stratosphere-troposphere exchange process and their plausible mechanisms, large uncertainties still exist about the stratospheric ozone intrusion into troposphere. These intrusions may be more prominent and frequent especially over sub-tropical latitudes such as Himalayan region and adjacent Tibetan plateau (Pan et al., 2014; Nath et al., 2016). The present study for the first time highlighted the importance of short period gravity waves generated by changes in wind flow over mountain topography and its effect on tropospheric and surface ozone concentration.

Strong upward vertical velocities during December 09, 2008 reveals the same picture that the mountain waves propagated vertically up to

the tropopause levels followed by downward velocities (upward-downward couplet) indicating that the gravity waves (wave breaking) are involved in the process of contributing to the tropopause folding (tropopause altitude dropped to ~10 km) favoring stratosphere-troposphere exchange processes. Moreover, our observations also show generation of shorter vertical wavelengths due to orography induced gravity waves which is a vital component in intense tropopause folding by the mode of wave breaking (Lamarque et al., 1996; Dhaka et al., 2006; Hocking et al., 2007). On the other hand, our observations also showed weakening or strong influence of the sub-tropical jet streams during the event as compared to other days which is not only another potential indicator for the intense tropopause folding but also associated with strong stratosphere-troposphere intrusions over sub-tropical latitudes (figure not shown here).

Ozone distribution maps depict clear indication of stratospheric intrusions into the troposphere with significant intensity. Also, upper tropospheric ozone showed an increment of 0.15 ± 0.03 ppmv which is almost double the usual background ozone concentration ($\sim 0.06 \pm 0.002$ ppmv) due to mountain wave activity. The enhanced upper-tropospheric ozone is descending further down to mid- and lower-tropospheric altitudes which could lead to environmental and radiative impacts over Himalayan region. The tropopause height (pressure) sharp decrease (increase) confirms that the conditions are very much conducive for stratosphere-troposphere exchange process responsible for the intrusion of lower stratospheric ozone rich air into upper- and mid-tropospheric ozone poor air thereby showing an enhancement in ozone over Himalayan region. Moreover, our observations also revealed that sudden increase in tropospheric and surface ozone followed by increase in overall tropopause temperature reiterating that the tropospheric ozone is a potential greenhouse gas. The temporal evolution of relative humidity during December 2008 also confirms the sharp decrease of relative humidity at tropopause altitudes during the event day indicating strong mixing of lower stratospheric ozone rich dry air to upper tropospheric humid air. However, increase of relative humidity before the event could be associated with the convection triggered moisture transport from lower troposphere to higher altitudes through mountain waves (Das, 2009; Kim et al., 2016). Our observations revealed that mountain waves may have modulated the tropopause triggering the STE process leading to the ozone transport not only to upper troposphere but further transport down to surface from stratosphere.

5. Summary

Stratosphere-troposphere ozone intrusion due to orography induced gravity wave is investigated over Himalayan region based on the satellite data and in-situ measurements for the first time. We summarize our findings as following.

1. Presence of mountain wave during December 08–11, 2008 over Himalayan region confirmed from radiance and temperature perturbations suggesting that the shorter vertical wavelength gravity waves propagated to upper tropospheric altitudes reaching tropopause region.
2. Wave breaking phenomena at the tropopause could lead to intense tropopause folding during the mountain wave event which is also associated with strong updrafts followed by downdrafts forming a couplet triggering stratosphere-troposphere exchange process over the Himalayan region.
3. Intrusion of ozone from lower stratosphere to upper troposphere is evident which was also reflected from in-situ observations of surface ozone.
4. Two-fold enhancement in surface ozone estimating the descent rate of ~4 km/day or higher reaching Nainital site on December 11 although the intrusion was observed on December 09 early hours.

The present study emphasized the importance of wave induced atmospheric dynamics causing STE process whose signature was also observed at the surface. At this juncture, it is essential to have more coordinated balloon-borne measurements of meteorological parameters along with vertical profiles of ozone along with modeling efforts to understand the plausible mechanisms responsible for decrease (increase) in stratospheric (tropospheric) ozone over tropical, mid and also in high-latitudes.

Supplementary data to this article can be found online at <http://dx.doi.org/10.1016/j.rse.2017.07.011>.

Acknowledgements

This work is supported by Aryabhata Research Institute of Observational Sciences (ARIES), Department of Science and Technology, Govt. of India. The data used in the present study is acquired from NASA's Science Mission Directorate and are archived and distributed by the Goddard Earth Sciences (GES) Data and Information Services Center (DISC). CALIPSO data were obtained by NASA Langley Research Center Atmospheric Science Data Center. We are also thankful to ECMWF re-analysis Research data analysis, computational and information systems laboratory team for providing us the datasets required for our analysis. TES level-2 data used in this study was obtained from the NASA Langley Research Center Atmospheric Sciences Data Center. We are grateful to COSMIC team for providing the temperature for our observational period. We thank both the reviewers for their constructive suggestions which helped us to improve the quality of the manuscript.

References

- Anthes, R.A., Bernhardt, P.A., Chen, Y., Cucurull, L., Dymond, K.F., Ector, D., et al., 2008. The COSMIC/Formosat/3 mission: early results. *Bull. Am. Meteorol. Soc.* 89, 313–333.
- Aumann, H.H., Chahine, M.T., Gautier, C., Goldberg, M.D., Kalnay, E., McMillin, L.M., et al., 2003. AIRS/AMSU/HSB on the Aqua mission: design, science objectives, data products, and processing systems. *IEEE Trans. Geosci. Remote Sens.* 41:253–264. <http://dx.doi.org/10.1109/TGRS.2002.808356>.
- Beer, R., 2006. TES on the Aura mission: scientific objectives, measurements and analysis overview. *IEEE Trans. Geosci. Remote Sens.* 44 (5):1102. <http://dx.doi.org/10.1109/TGRS.2005.863716>.
- Beer, R., Glavich, T.A., Rider, D.M., 2001. Tropospheric emission spectrometer for the Earth Observing System's Aura satellite. *Appl. Opt.* 40:2356–2367. <http://dx.doi.org/10.1364/AO.40.002356>.
- Bian, J., 2009. Features of ozone mini-hole events over the Tibetan Plateau. *Adv. Atmos. Sci.* 26 (2), 305–311.
- Bowman, K.W., Rodgers, C.D., Kulawik, S.S., Worden, J., Sarkissian, E., Osterman, G., et al., 2006. Tropospheric emission spectrometer: retrieval method and error analysis. *IEEE Trans. Geosci. Remote Sens.* 44 (5):1297–1307. <http://dx.doi.org/10.1109/TGRS.2006.871234>.
- Chand, D., Modh, K.S., Naja, M., Venkataramani, S., Lal, S., 2001. Latitudinal trends in O₃, CO, CH₄, SF₆, over the Indian Ocean during the INDOEX I/P-1999 ship cruise. *Curr. Science* 80, 100–104.
- Chen, X.L., Ma, Y.M., Kelder, H., Su, Z., Yang, K., 2011. On the behaviour of the tropopause folding events over the Tibetan Plateau. *Atmos. Chem. Phys.* 11:5113–5122. <http://dx.doi.org/10.5194/acp-11-5113-2011>.
- Cracknell, A.P., Varotsos, C.A., 1994. Ozone depletion over Scotland as derived from Nimbus-7 TOMS measurements. *Int. J. Remote Sens.* 15 (13), 2659–2668.
- Cracknell, A.P., Varotsos, C.A., 1995. The present status of the total ozone depletion over Greece and Scotland: a comparison between Mediterranean and more northerly latitudes. *Int. J. Remote Sens.* 16 (10), 1751–1763.
- Cracknell, A.P., Varotsos, C.A., 2011. New aspects of global climate-dynamics research and remote sensing. *Int. J. Remote Sens.* 32 (3), 579–600.
- Crutzen, P.J., 1995. Ozone in the troposphere. In: Singh, H.B. (Ed.), *Composition, Chemistry and Climate of the Atmosphere*. Van Nostrand-Reinhold, New York, pp. 349–393.
- Das, S.S., 2009. A new perspective on MST radar observations of stratospheric intrusions into troposphere associated with tropical cyclone. *Geophys. Res. Lett.* 36:L15821. <http://dx.doi.org/10.1029/2009GL039184>.
- Das, S.S., Ratnam, M.V., Uma, K.N., Subrahmanyam, K.V., Girach, I.A., Patra, A.K., et al., 2016a. Influence of tropical cyclones on tropospheric ozone: possible implication. *Atmos. Chem. Phys.* 16:4837–4847. <http://dx.doi.org/10.5194/acp-16-4837-2016>.
- Das, S.S., Ratnam, M.V., Uma, K.N., Patra, A.K., Subrahmanyam, K.V., Girach, I.A., et al., 2016b. Stratospheric intrusion into the troposphere during the tropical cyclone Nilam (2012). *Q. J. R. Meteorol. Soc.* <http://dx.doi.org/10.1002/qj.2810>.
- David, L.M., Nair, P.R., 2013. Tropospheric column O₃ and NO₂ over the Indian region observed by Ozone Monitoring Instrument (OMI): seasonal changes and long-term trends. *Atmos. Environ.* 65:25–39. <http://dx.doi.org/10.1016/j.atmosenv.2012.09.033>.

- David, L.M., Nair, P.R., 2011. Diurnal and seasonal variability of surface ozone and NO_x at a tropical coastal site: Association with mesoscale and synoptic meteorological conditions. *J. Geophys. Res.* 116, D10303. <http://dx.doi.org/10.1029/2010JD015076>.
- Dee, D.P., Uppala, S.M., Simmons, A.J., Berrisford, P., Poli, P., Kobayashi, S., et al., 2011. The ERA-Interim reanalysis: configuration and performance of the data assimilation system. *Q. J. R. Meteorol. Soc.* 137:553–597. <http://dx.doi.org/10.1002/qj.828>.
- Dhaka, S.K., Yamamoto, M.K., Shibagaki, Y., Hashiguchi, H., Fukao, S., Chun, H.-Y., 2006. Equatorial Atmosphere Radar observations of short vertical wavelength gravity waves in the upper troposphere and lower stratosphere region induced by localized convection. *Geophys. Res. Lett.* 33:L19805. <http://dx.doi.org/10.1029/2006GL027026>.
- Durran, D.R., 1986. Mountain waves. In: Ray, P. (Ed.), *Mesoscale Meteorology and Forecasting*. Am. Meteorol. Soc., Boston, Mass., pp. 472–492.
- Efstathiou, M.N., Varotsos, C.A., 2010. On the altitude dependence of the temperature scaling behaviour at the global troposphere. *Int. J. Remote Sens.* 31 (2), 343–349.
- Fritts, D.C., Rastogi, P.K., 1985. Convective and dynamical instabilities due to gravity wave motions in the lower and middle atmosphere: Theory and observations. *Radio Sci.* 20 (6):1247–1277. <http://dx.doi.org/10.1029/RS020i006p01247>.
- Ghude, S.D., Chate, D.M., Jena, C., Beig, G., Kumar, R., Barth, M.C., et al., 2016. Premature mortality in India due to PM_{2.5} and ozone exposure. *Geophys. Res. Lett.* 43: 4650–4658. <http://dx.doi.org/10.1002/2016GL068949>.
- Girach, I.A., Ojha, N., Prabha, R., Nair, Pozzer A., Tiwari, Y.K., Ravi, Kumar K., et al., 2017. Variations in O₃, CO, and CH₄ over the Bay of Bengal during the summer monsoon season: shipborne measurements and model simulations. *Atmos. Chem. Phys.* 17: 257–275. <http://dx.doi.org/10.5194/acp-17-257-2017>.
- Hocking, W.K., Smith, T.C., Tarasick, D.W., Argall, P.S., Strong, K., Rochon, Y., et al., 2007. Detection of stratospheric ozone intrusions by wind profiler radars. *Nature* 450: 281–284. <http://dx.doi.org/10.1038/nature06312>.
- Holton, J.R., Haynes, P.H., McIntyre, M.E., Douglass, A.R., Rood, R.B., Pfister, L., 1995. Stratosphere-troposphere exchange. *Rev. Geophys.* 33 (4):403–439. <http://dx.doi.org/10.1029/95RG02097>.
- Hoskins, B.J., McIntyre, M.E., Robertson, W., 1985. On the use and significance of isentropic potential vorticity map. *Q. J. R. Meteorol. Soc.* 111:877–946. <http://dx.doi.org/10.1256/smsqj.47001>.
- IPCC, 2013. *Climate change 2013: the physical science basis*. In: Stocker, T., Qin, D., Plattner, G., Tignor, M., Allen, S., Boschung, J., Nauels, A., Xia, Y., Bex, V., Midgley, P. (Eds.), *Contribution of Working Group I to the Fifth Assessment Report of the Intergovernmental Panel on Climate Change*. Cambridge University Press, Cambridge, UK, pp. 1–1535.
- Kaifler, B., Kaifler, N., Ehard, B., Dörnbrack, A., Rapp, M., Fritts, D.C., 2015. Influences of source conditions on mountain wave penetration into the stratosphere and mesosphere. *Geophys. Res. Lett.* 42:9488–9494. <http://dx.doi.org/10.1002/2015GL066465>.
- Kim, J.-E., Alexander, M.J., Bui, T.P., Dean-Day, J.M., Lawson, R.P., Woods, S., et al., 2016. Ubiquitous Influence of Waves on Tropical High Cirrus Cloud. *Geophys. Res. Lett.* 43:5895–5901. <http://dx.doi.org/10.1002/2016GL069293>.
- Kleinman, L., Lee, Y.-N., Springston, S.R., Nunnermacker, L., Zhou, X., Brown, R., et al., 1994. Ozone formation at a rural site in the southern United States. *J. Geophys. Res.* 99: 3469–3482. <http://dx.doi.org/10.1029/93JD02991>.
- Kulawik, S.S., Worden, J., Eldering, A., Bowman, K., Gunson, M., Osterman, G.B., et al., 2006. Implementation of cloud retrievals for Tropospheric Emission Spectrometer (TES) atmospheric retrievals: 1. Description and characterization of errors on trace gas retrievals. *J. Geophys. Res.* 111:D24204. <http://dx.doi.org/10.1029/2005JD006733>.
- Kumar, R., Naja, M., Pfister, G.G., Barth, M.C., Brasseur, G.P., 2013. Source attribution of carbon monoxide in India and surrounding regions during wintertime. *J. Geophys. Res.-Atmos.* 118 (4), 1981–1995.
- Kumar, R., Naja, M., Sathesh, S.K., Ojha, N., Joshi, H., Sarangi, T., et al., 2011. Influences of the springtime northern Indian biomass burning over the central Himalayas. *J. Geophys. Res.* 116, D19302. <http://dx.doi.org/10.1029/2010JD015509>.
- Kumar, R., Naja, M., Venkataramani, S., Wild, O., 2010. Variations in surface ozone at Nainital: A high-altitude site in the central Himalayas. *J. Geophys. Res.* 115, D16302. <http://dx.doi.org/10.1029/2009JD013715>.
- Kursinski, E.R., Hajj, G.A., Schofield, J.T., Linfield, R.P., Hardy, K.R., 1997. Observing Earth's atmosphere with radio occultation measurements using the Global Positioning System. *J. Geophys. Res.* 102, 23429–23466.
- Lal, S., Venkataramani, S., Srivastava, S., Gupta, S., Mallik, C., Naja, M., 2013. Transport effects on the vertical distribution of tropospheric ozone over the tropical marine regions surrounding India. *J. Geophys. Res.* 118 (3), 1513–1524.
- Lamarque, J.-F., Langford, A.O., Proffitt, M.-H., 1996. Cross-tropopause mixing of ozone through gravity wave breaking: observation and modelling. *J. Geophys. Res.* 101 (D17), 22969–22976.
- Lelieveld, J., Evans, J.S., Fnais, M., Giannadaki, D., Pozzer, A., 2015. The contribution of outdoor air pollution sources to premature mortality on a global scale. *Nature* 525: 367–371. <http://dx.doi.org/10.1038/nature15371>.
- Levy II, H., Mahlman, J.D., Moxim, W.J., Liu, S.C., 1985. Tropospheric ozone: The role of transport. *J. Geophys. Res.* 90, 3753–3772.
- Logan, A.Z., 1985. Tropospheric ozone: Seasonal behavior, trends, and anthropogenic influence. *J. Geophys. Res.* 90:10,463–10,482. <http://dx.doi.org/10.1029/JD090iD06p10463>.
- Lyapustin, A., Alexander, M.J., Ott, L., Molod, A., Holben, B., Susskind, J., et al., 2014. Observation of mountain lee waves with MODIS NIR column water vapor. *Geophys. Res. Lett.* 41:710–716. <http://dx.doi.org/10.1002/2013GL058770>.
- Naja, M., Lal, S., 1996. Changes in surface ozone amount and its diurnal and seasonal patterns, from 1954–55 to 1991–93, measured at Ahmedabad (23 N), India. *Geophys. Res. Lett.* 23 (1), 81–84.
- Naja, M., Chand, D., Sahu, L., Lal, S., 2004. Trace gases over marine region around India. *Indian J. Mar. Sci.* 33 (1), 95–106.
- Naja, M., Bhardwaj, P., Singh, N., Kumar, P., Kumar, R., Ojha, N., et al., 2016. High-frequency vertical profiling of meteorological parameters using AMF1 facility during RAWEX–GVAX at ARIES, Nainital. *Curr. Sci.* 111, 132–140.
- Nath, D., Chen, W., Graf, H.-F., Lan, X., Gong, H., Nath, R., et al., 2016. Subtropical potential vorticity intrusion drives increasing tropospheric ozone over the tropical Central Pacific. *Sci Rep* 6:21370. <http://dx.doi.org/10.1038/srep21370>.
- Niranjan Kumar, K., Ramkumar, T.K., 2008. Characteristics of inertia-gravity waves over Gadanki during the passage of a deep depression over the Bay of Bengal. *Geophys. Res. Lett.* 35, L13804. <http://dx.doi.org/10.1029/2008GL033937>.
- Niranjan Kumar, K., Ramkumar, T.K., Krishnaiah, M., 2011. Vertical and lateral propagation characteristics of intraseasonal oscillation from the tropical lower troposphere to upper mesosphere. *J. Geophys. Res.* 116, D21112. <http://dx.doi.org/10.1029/2010JD015283>.
- Niranjan Kumar, K., Ramkumar, T.K., Krishnaiah, M., 2012. Analysis of large-amplitude stratospheric mountain wave event observed from the AIRS and MLS sounders over the western Himalayan region. *J. Geophys. Res.* 117:D22102. <http://dx.doi.org/10.1029/2011JD017410>.
- Niranjan Kumar, K., Phanikumar, D.V., Ouarda, T.B.M.J., Rajeevan, M., Naja, M., Shukla, K.K., 2016. Modulation of surface meteorological parameters by extratropical planetary-scale Rossby waves. *Ann. Geophys.* 34:123–132. <http://dx.doi.org/10.5194/angeo-34-123-2016>.
- Ojha, N., Naja, M., Sarangi, T., Kumar, R., Bhardwaj, P., Lal, S., et al., 2014. On the processes influencing the vertical distribution of ozone over the central Himalayas: analysis of yearlong ozonesonde observations. *Atmos. Environ.* 88, 201–211.
- Pan, L.L., Homeyer, C.R., Honomichl, S., Ridley, B.A., Weisman, M., Barth, M.C., Hair, J.W., Fenn, M.A., Butler, C., Diskin, G.S., Crawford, J.H., Ryerson, T.B., Pollack, I., Peischl, J., Huntrieser, H., 2014. Thunderstorms enhance tropospheric ozone by wrapping and shedding stratospheric air. *Geophys. Res. Lett.* 41 (22):7785–7790. <http://dx.doi.org/10.1002/2014GL061921>.
- Pathakoti, M., Karri, S.R., SVS, S.K., PVN, R., CBS, D., 2016. Evidence of stratosphere-troposphere exchange during severe cyclones: a case study over Bay of Bengal, India. *Geomat. Nat. Haz. Risk* 7 (6), 1816–1823.
- Rodgers, C., 2000. *Inverse Methods for Atmospheric Sounding: Theory and Practice*. World Sci., Hackensack, N. J.
- Sarangi, T., Naja, M., Ojha, N., Kumar, R., Lal, S., Venkataramani, S., et al., 2014. First simultaneous measurements of ozone, CO, and NO_y at a high-altitude regional representative site in the central Himalayas. *J. Geophys. Res.-Atmos.* 119 (3), 1592–1611.
- Shukla, K.K., Phanikumar, D.V., Newsom, R.K., Niranjan, Kumar K., Venkat Ratnam, M., Naja, M., et al., 2014. Estimation of the mixing layer height over a high altitude site in Central Himalayan region by using Doppler lidar. *J. Atmos. Sol. Terr. Phys.* 109, 48–53.
- Stevenson, D.S., Dentener, F.J., Schultz, M.G., Ellingsen, K., van Noije, T.P.C., Wild, O., et al., 2006. Multi-model ensemble of present-day and near-future tropospheric ozone. *J. Geophys. Res.* 111:D8301. <http://dx.doi.org/10.1029/2005JD006338>.
- Susskind, J., Barnett, C.D., Blaisdell, J.M., 2003. Retrieval of atmospheric and surface parameters from AIRS/AMSU/HSB data in the presence of clouds. *IEEE Trans. Geosci. Remote Sens.* 41:390–409. <http://dx.doi.org/10.1109/Tgrs.2002.808236>.
- Tobo, Y., Iwasaka, Y., Zhang, D., Shi, G., Kim, Y.-S., Tamura, K., et al., 2008. Summertime “ozone valley” over the Tibetan Plateau derived from ozonesondes and EP/TOMS data. *Geophys. Res. Lett.* 35:L16801. <http://dx.doi.org/10.1029/2008GL034341>.
- Varotsos, C.A., Cracknell, A.P., 1994. Three years of total ozone measurements over Athens obtained using the remote sensing technique of a Dobson spectrophotometer. *Int. J. Remote Sens.* 15 (7), 1519–1524.
- Varotsos, C., Kalabokas, P., Chronopoulos, G., 1994. Association of the laminated vertical ozone structure with the lower-stratospheric circulation. *J. Appl. Meteorol.* 33 (4): 473–476. [http://dx.doi.org/10.1175/1520-0450\(1994\)033<0473:O.CO>2](http://dx.doi.org/10.1175/1520-0450(1994)033<0473:O.CO>2).
- Worden, J., Kulawik, S.S., Shephard, M.W., Clough, S.A., Worden, H., Bowman, K., et al., 2004. Predicted errors of Tropospheric Emission Spectrometer nadir retrievals from spectral window selection. *J. Geophys. Res.* 109:D09308. <http://dx.doi.org/10.1029/2004JD004522>.
- World Health Organization, 2012. *World Health Organization Statistical Information System (WHOSIS), Detailed Data Files of the WHO Mortality Database*. (http://www.who.int/healthinfo/statistics/mortality_rawdata/en/) (WHO, Geneva, 2012).
- Zeng, G., Pyle, J.A., Young, P.J., 2008. Impact of climate change on tropospheric ozone and its global budgets. *Atmos. Chem. Phys.* 8, 369–387.
- Zhou, S., Zhang, R., 2005. Decadal variations of temperature and geopotential height over the Tibetan Plateau and their relations with Tibet ozone depletion. *Geophys. Res. Lett.* 32:L18705. <http://dx.doi.org/10.1029/2005GL023496>.